ACS Medicinal Chemistry Letters

Letter

pubs.acs.org/acsmedchemlett

# Iron Chelators in Photodynamic Therapy Revisited: Synergistic Effect by Novel Highly Active Thiosemicarbazones

Anna Mrozek-Wilczkiewicz,[†,‡] Maciej Serda,[†] Robert Musiol,[†] Grzegorz Malecki,[†] Agnieszka Szurko,[‡] Angelika Muchowicz,[§] Jakub Golab,[§] Alicja Ratuszna,[‡] and Jaroslaw Polanski*[,†]

[†]Institute of Chemistry, University of Silesia, Szkolna 9, PL-40-006 Katowice, Poland

[‡]Institute of Physics, University of Silesia, Uniwersytecka 4, PL-40-007 Katowice, Poland

[§]Center of Biostructure Research, Medical University of Warsaw, Banacha 1a, PL-02-097 Warsaw, Poland

Supporting Information

**ABSTRACT:** In photodynamic therapy (PDT), a noninvasive anticancer treatment, visible light, is used as a magic bullet selectively destroying cancer cells by a photosensitizer that is nontoxic in the dark. Protoporphyrin IX (PpIX) is a natural photosensitizer synthesized in the cell, which is also a chelating agent that if bonded to $Fe^{2+}$ forms heme, a central component of hemoglobin. Therefore, xenobiotic iron chelators can disturb iron homeostasis, increasing the accumulation of PpIX, obstructing the last step of heme biosynthesis, and enhancing PDT efficiency. However, the attempts to use this promising idea have not proved to be hugely successful. Herein, we revisited this issue by analyzing the application of iron chelators highly toxic in the dark, which should have higher $Fe^{2+}$ affinity than the nontoxic chelators used so far. We have designed and prepared thiosemicarbazones (TSC) with the highest dark cellular cytotoxicity among TSCs ever reported. We demonstrate that compound **2** exerts powerful PDT enhancement when used in combination with 5-aminolevulinic acid (ALA), a precursor of PpIX.

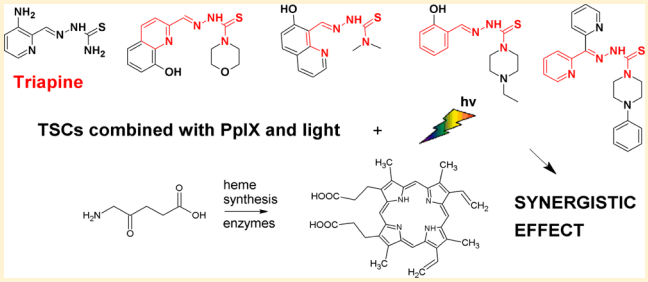


**KEYWORDS:** *Photodynamic therapy, thiosemicarbazones, protoporphyrin IX, triapine, reactive oxygen species*

Desferrioxamine (DFO, Figure 1, **I**) is an iron chelating drug that has been registered recently for the treatment of iron overload diseases.[1] Applications of DFO, thiosemicarbazones (TSCs), or other iron chelators have been widely investigated as potential anticancer therapeutic agents;[2,3] however, triapine (Figure 1, **II**) is the first TSC that has entered phase 2 clinical trials as a drug candidate for these conditions.[4] Several paradigms have been proposed to explain the molecular mechanisms involved in the activity of these compounds,[5] including triapine itself,[6] with the hope of obtaining FDA approval. Potential cytostatic/cytotoxic mechanisms of TSCs include inhibition of cellular iron uptake from transferrin,[7] mobilization of iron from cells, inhibition of ribonucleotide reductase, the iron-containing enzyme involved in the rate-limiting step of DNA synthesis,[8] and formation of reactive oxygen species (ROS).[9] The latter mechanism is significant in light of recent reports of the role of ROS generation in increasing the chelator activity against tumor cells.[5,10]

The essence of PDT[11] is based on producing singlet oxygen and free radicals in a reaction triggered by excitation of the photosensitizer (PS) by light of appropriate wavelength. The variety among PSs or their prodrugs offers good activity and selectivity.[12] Among them, 5-aminolevulinic acid (ALA) and its derivatives, which are precursors of protoporphyrin IX (PpIX), are used commonly.[13] Exogenous addition of ALA bypasses the normal negative feedback mechanisms and causes the accumulation of PpIX in the tissue.[14] The accumulation of PS in malignant tissue is of clinical importance allowing for increased treatment selectivity. The difference in accumulation of PpIX in diseased as compared to healthy tissue results from abnormal activity of enzymes regulating the formation of PpIX (porphobilinogen deaminase) and heme (ferrochelatase) in cancer cells.[15] This phenomenon is the basis of the concept of combination therapy, where iron chelators are used as adjuvants in ALA-PDT.[16] The use of nontoxic iron chelators deprives the cells of $Fe^{2+}$ crucial for the last step of heme biosynthesis, thereby increasing the accumulation of PpIX. Although successful application of iron chelators in PDT is a promising idea, the achieved synergy levels in such strategies have been relatively low so far.[17] Minimized dark cytotoxicity of the PS, including iron chelator enhancement, is considered to be a substantial prerequisite for the safety of PDT.[18]

Herein, we present novel thiosemicarbazones (Figure 1) with the highest dark cellular cytotoxicity among all previously reported TSCs. We demonstrate that compound **1** exerts

**Received:** October 24, 2013
**Accepted:** January 23, 2014
**Published:** January 23, 2014

   dx.doi.org/10.1021/ml400422a | ACS Med. Chem. Lett. 2014, 5, 336−339

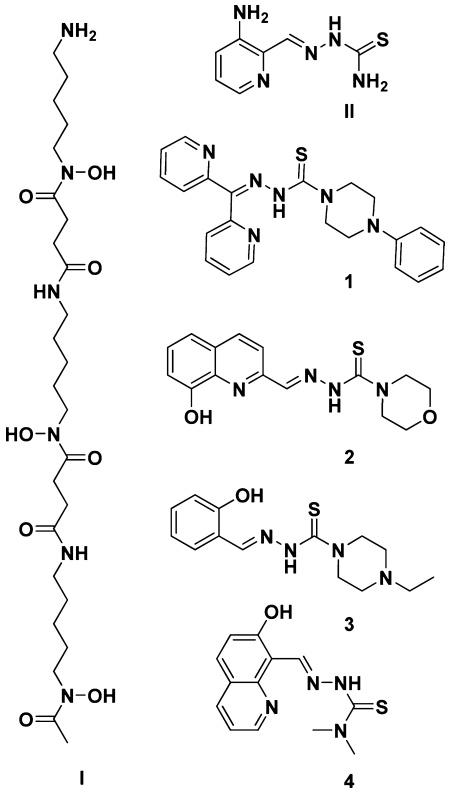


**Figure 1.** Structures of the TSCs (**1**–**4**), DFO (**I**), and triapine (**II**).

powerful photocytotoxic activity when used in combination with ALA-PDT. Very strong activity was also observed under these conditions for compound **2**, which exerts slightly lower dark cytotoxicity, but with an $IC_{50}$ value still in the nanomolar range. On the contrary, little to no synergy was observed for low activity TSC compounds **3**–**4** and for reference compounds DFO (**I**) or triapine (**II**) under similar conditions. At the same time, the synergy level described by the combination index (CI) does not correlate closely to the dark cytotoxicity of the compounds.

TSCs were synthesized by reacting equimolar amounts of the respective (hetero)aromatic ketones or carbaldehydes and thiosemicarbazide under microwave irradiation (closed vessel mode). The reactions were carried out in EtOH with a catalytic amount of acetic acid (Scheme 1). Products were isolated by crystallization and purified by column chromatography (Figure S1 in the Supporting Information). For characterization data, see Supporting Information (Figure S2–S4).

**Scheme 1**

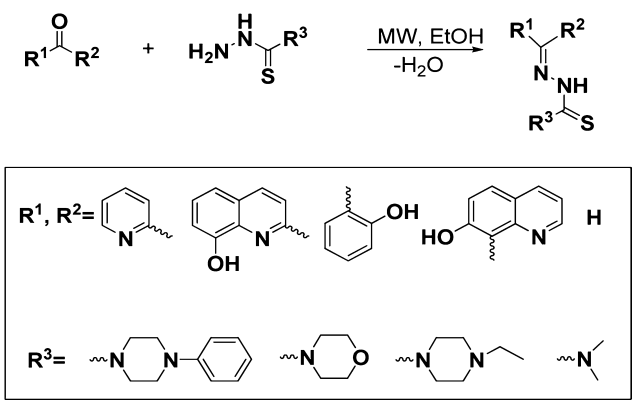


Compound **1** was structurally characterized by single-crystal X-ray. The compound crystallized in the monoclinic $P2_1/c$ space group (Table S1 and Figure S5 in the Supporting Information); CCDC 908257 contains the supplementary crystallographic data, freely available at http://www.ccdc.cam.ac.uk/conts/retrieving.html or from the Cambridge Crystallographic Data Centre, 12 Union Road, Cambridge CB2 1EZ, UK; fax +44 1223–336–033 or e-mail deposit@ccdc.cam.ac.uk). In the structure of the compound, the thione sulfur atom S(1) was cis disposed with respect to the azomethine nitrogen atom N(2). The C(1)–S(1) bond length of 1.669(2) Å was adequate to form a carbon–sulfur double bond. The N(1)–H(1) group was capable of acting as a H-donor, with the N(5) of the pyridine ring acting as the acceptor in the intramolecular hydrogen bond formation. Moreover, in the structure of the compound $\pi$-stacking interactions between the aromatic (phenyl and pyridine) rings were visible but distances of 3.565 and 3.913 Å indicated rather weak interactions.

Dark cytotoxicity of **1**–**4** and **I** was studied using HCT 116 colorectal carcinoma cells with wild-type (+/+) or deleted (−/−) tumor suppressor TP53 gene. The p53 is tumor suppressor responsible for induction of the apoptosis. It may regulate the ROS formation in the cells acting as both pro- or antioxidant.[19] Furthermore, after oxidative stress its activity may increase leading to cell death. Thus, we decided to involve these p53 positive and negative cells into consideration. Raji and HeLa cell lines were used for the additional characterization of cytostatic/cytotoxic effects of investigated compounds, while normal human-derived fibroblasts (NHDF) were used to investigate the selectivity of cytostatic/cytotoxic activity among cancer and normal cells. In an evaluation of $IC_{50}$ values (Table 1), we observed that compound **1** showed the highest activity against the tested cells, with $IC_{50}$ values of 0.81 and 0.76 nM against HCT 116+/+ and HCT 116−/−, respectively. The Raji cells were even more susceptible to compound **1**, with ∼2.4-fold lower $IC_{50}$ value. In contrast to compound **1**, which displayed high toxicity against normal NHDF cells ($IC_{50}$ = 1.73 nM), compound **2**, based on the quinoline moiety, exhibited a differential effect, inhibiting the HCT 116 cancer cell line with an $IC_{50}$ value that was 2770-fold more potent than that for NHDF cells in the dark cytotoxicity tests.

Fluorescence intensity time profile of PpIX assembly in HCT 116+/+ cells growing in medium supplemented with ALA is presented in Figure S6 (see Supporting Information). The experiments were performed in medium deprived of phenol red so as not to coincide with the radiation activating PpIX, under the reduced light intensity.

The addition of ALA led to a steady increase in the PpIX concentration, which reached a plateau after 18–24 h. These experiments allowed us to determine the optimal incubation time for the cells cultured with ALA. The maximal concentration of PpIX was achieved after about 24 h after which no further PpIX increase was observed. During the whole test (74 h), viability of the cells was confirmed using the MTS assay. Since serum suppresses the fluorescence signal due to PpIX binding to proteins,[20] the cells were cultured in serum-free medium; however, it did not affect their proliferation to a large extent. ALA concentration, which was optimized in the other series of tests, was set to 1 mM. The influence of TSCs on the cellular PpIX formation was tested under different TSC concentrations for various incubation times. The experiments


dx.doi.org/10.1021/ml400422a | ACS Med. Chem. Lett. 2014, 5, 336–339

Table 1. Dark- and Photocytotoxicity in ALA-PDT-TSC Treatment for Compounds 1−4 and I

| | toxicity[a] $IC_{50}$ ($\mu$M) | | | | |
|---|---|---|---|---|---|
| | 1 | 2 | 3 | 4 | DFO (I) |
| HCT116 +/+ | 0.00081 ± 0.00013 | 0.00384 ± 0.00146 | >20 | >20 | >200 |
| HCT116 −/− | 0.00076 ± 0.00007 | 0.01677 ± 0.00558 | >20 | >2o | >200 |
| Raji | 0.00032 ± 0.00003 | 0.02123 ± 0.00568 | >10 | nd[b] | nd |
| HeLa | 0.57 ± 0.16 | 0.176 ± 0.007 | >20 | nd | nd |
| NHDF | 0.00173 ± 0.00071 | >10 | >20 | >20 | nd |
| CI[c] | 0.47 | 0.08 | 0.95 | 6.08 | 1.01 |

[a]$IC_{50}$ values for triapine (II) used as reference compound: 1.226 ± 0.136 (HCT 116+/+). CI values for triapine: 0.85 (HCT 116+/+). [b]nd: not determined. [c]ALA-TSC-PDT combination therapy; CI, combination index. For detailed calculations, compare Supporting Information.

indicated that the TSC addition did not influence formation of PpIX in cultured HCT 116+/+ cells (data not shown). For highly active TSCs, the concentration of each compound did not exceed a nanomolar scale. Therefore, the potential to form an iron complex with TSC is extremely low, which suggests that this level iron−TSC complex is not high enough to produce a noticeable effect in the synthesis of heme. Similarly, no increase in PpIX concentration was observed for dark nontoxic TSCs **3**, **4**, or **I** at much higher concentrations of ca. 50 $\mu$M. In turn, greater concentrations of toxic TSCs **1** and **2** resulted in cell death.

Photocytotoxic behavior of TSCs in the combined ALA-PDT-TSC experiment was determined as presented in Table 1. Interactions between irradiated PpIX (given as light dose at constant ALA concentration = 1 mM) and TSC (as concentration) were measured according to Chou−Thalay method.[21] Increasing the doses in a constant manner we calculated the combination index (CI) as a ratio of the sum of the doses in TSC or ALA-PDT to the doses of each therapy alone, having the same cytotoxic effect[22] (see Supporting Information for the detailed combination of doses, Table S2). A value of CI below 1 indicates synergy, CI amounting to 1 indicates an additive effect, whereas the CI value greater than 1 implies antagonism. A combination of compound **2** with ALA-PDT yielded a significant synergy, CI = 0.08, at a nanomolar concentration of **2**. Moreover, CI appeared to be stable for compound **2** over the whole range of tested light doses (PDT) and TSC concentrations. This means that the concentration of TSC **2** can be reduced by almost 60-fold to achieve a result comparable to its effect if used alone at the light dose of 9.8 J/cm$^2$, or alternatively, the light dose can be reduced by ca. 4 times in the combination treatment with TSC **2** at a concentration level of 11 nM. This flexibility offers the potential to minimize side effects while maintaining the drug efficacy. These conclusions are based on calculations of DRI (dose reduction index) according to the Chou−Thalay method (data not shown).[21] For compound **1**, a weaker synergy was observed. Compounds **3** and **I** seemed to act independently from PDT, and a value consistent with additivity could be observed in this case. In contrast, compound **4** displayed an antagonism with PDT. In case of triapine (**II**), we detected very weak synergy (CI value equal to 0.85).

The results of these experiments indicated that TSC can influence photocytotoxic behavior in the combined ALA-PDT-TSC regimen. Moreover, subnanomolar concentrations of TSC do not appear to be high enough to deprive the cellular mechanism of iron through simple chelation. To test this proposal, we tested the influence of the addition of exogenous iron ($FeCl_3$). Hypothetically, the excess of iron competes with the ability of TSC to chelate heme iron, reducing PpIX and favoring heme content. Surprisingly, in our experiment, an excess of iron did not affect photocytotoxic behavior of the tested TSCs (see Supporting Information). This result suggested that TSCs did not affect heme synthesis by iron chelation as suggested in many publications.[23,24] The decrease of ferrochelatase expression in HCT 116 cells[25,26] can be one of the factors influencing this atypical behavior.

As cytostatic/cytotoxic mechanisms of TSCs can include a number of effects during ALA-PDT-TSC treatment, we additionally confirmed the formation of ROS. The positive results of these experiments indicated generation of ROS in HCT 116+/+ cells by the compounds **1**, **2**, and **II** (Figure S7 in the Supporting Information). Thus, a synergistic effect can be additionally enhanced by the coexistence of two direct cytotoxic effects; the first resulting from a typical PDT triggered by a PS produced endogenously and, regardless of this event, the formation of ROS by TSC in the Fenton reaction.

In conclusion, a significantly potentiated photocytotoxicity is observed when TSC compounds **1** and **2** are used in combination with ALA-PDT. Compound **2** appears to be the most effective in the combination therapy studies, revealing the highest selectivity in terms of relatively low dark cytotoxicity against normal NHDF cells. The similarity of the studied TSCs to triapine, the new important drug candidate in phase 2 clinical trials, makes the observed effects worthy of careful attention. These studies reveal novel applications for TSCs and offer better understanding of the intracellular targeting mechanisms of TSCs. Further studies on the larger series of TSCs as well as potential applications of triapine are in progress.

## ■ ASSOCIATED CONTENT

### Supporting Information

Spectroscopic characterization data, figures, tables, graphs, and detailed description of experimental procedures. This material is available free of charge via the Internet at http://pubs.acs.org.

## ■ AUTHOR INFORMATION


### Corresponding Author

*(J.P.) E-mail: polanski@us.edu.pl.


### Author Contributions

The manuscript was written through contributions of all authors. All authors have given approval to the final version of the manuscript.


### Funding

J.P. is supported by the NCBiR Warsaw PBS2/A5/40/2014. A.M.-W. appreciates the support of the NCN grant N405/068440 and the DoktoRIS studentship. M.S. was supported by a TWING scholarship and by NCN grant DEC-2011/01/N/NZ4/01166. J.G. was supported by a grant from the European

Commission seventh Framework Programme: FP7-REGPOT-2012-CT2012-316254-BASTION. A.M. is a recipient of the Polish L'Oréal-UNESCO Awards for Women in Science. R.M. acknowledges the NCN grant 2013/09/B/NZ7/00423.

### Notes

The authors declare no competing financial interest.

## ■ ABBREVIATIONS

PDT, photodynamic therapy; PpIX, protoporphyrin IX; TSC, thiosemicarbazones; ALA, 5-aminolevulinic acid; DFO, desferrioxamine; ROS, reactive oxygen species; PS, photosensitizer; CI, combination index; DRI, dose reduction index

## ■ REFERENCES

(1) Lui, G. Y. L.; Obeidy, P.; Ford, S. J.; Tselepis, C.; Sharp, D. M.; Jansson, P. J.; Kalinowski, D. S.; Kovacevic, Z.; Lovejoy, D. B.; Richardson, D. R. The iron chelator, deferasirox, as a novel strategy for cancer treatment: oral activity against human lung tumor xenografts and molecular mechanism of action. *Mol. Pharmacol.* **2013**, *83*, 179−190.

(2) Yuan, J.; Lovejoy, D. B.; Richardson, D. R. Novel di-2-pyridyl-derived iron chelators with marked and selective antitumor activity: in vitro and in vivo assessment. *Blood* **2004**, *104*, 1450−1458.

(3) Richardson, D. R.; Milnes, K. The potential of iron chelators of the pyridoxalisonicotinoyl hydrazone class as effective antiproliferative agents II: the mechanism of action of ligands derived from salicylaldehyde benzoyl hydrazone and 2-hydroxy-1-naphthylaldehyde benzoyl hydrazine. *Blood* **1997**, *89*, 3025−3038.

(4) Ocean, A. J.; Christos, P.; Sparano, J. A.; Matulich, D.; Kaubish, A.; Siegel, A.; Sung, M.; Ward, M. M.; Hamel, N.; Espinoza-Delgado, I.; Yen, Y.; Lane, M. E. Phase II trial of the ribonucleotidereductase inhibitor 3-aminopyridine-2-carboxaldehydethiosemicarbazone plus gemcitabine in patients with advanced biliary tract cancer. *Cancer Chemother. Pharmacol.* **2011**, *68*, 379−388.

(5) Yu, Y.; Kalinowski, D. S.; Kovacevic, Z.; Siafakas, A. R.; Jansson, P. J.; Stefani, C.; Lovejoy, D. B.; Sharpe, P. C.; Bernhardt, P. V.; Richardson, D. R. Thiosemicarbazones from the old to new: iron chelators that are more than just ribonucleotide reductase inhibitors. *J. Med. Chem.* **2009**, *52*, 5271−5294.

(6) Aye, Y.; Long, M. J. C.; Stubbe, J. Mechanistic studies of semicarbazonetriapine targeting human ribonucleotide reductase in vitro and in mammalian cells: tyrosyl radical quenching not involving reactive oxygen species. *J. Biol. Chem.* **2012**, *287*, 35768−35778.

(7) Evans, R. W.; Kong, X.; Hider, R. C. Iron mobilization from transferrin by therapeutic iron chelating agents. *Biochim. Biophys. Acta* **2012**, *1820*, 282−290.

(8) Thelander, L.; Gräslund, A.; Thelander, M. Continual presence of oxygen and iron required for mammalian ribonucleotide reduction: possible regulation mechanism. *Biochem. Biophys. Res. Commun.* **1983**, *110*, 859−865.

(9) Kalinowski, D. S.; Richardson, D. R. The evolution of iron chelators for the treatment of iron overload disease and cancer. *Pharmacol. Rev.* **2005**, *57*, 547−583.

(10) Kalinowski, D. S.; Yu, Y.; Sharpe, P. C.; Islam, M.; Liao, Y.-T.; Lovejoy, D. B.; Kumar, N.; Bernhardt, P. V.; Richardson, D. R. Design, synthesis, and characterization of novel iron chelators: structure-activity relationships of the 2-benzoylpyridine thiosemicarbazone series and their 3-nitrobenzoyl analogues as potent antitumor agents. *J. Med. Chem.* **2007**, *50*, 3716−3729.

(11) Agostinis, P.; Berg, K.; Cengel, K. A.; Foster, T. H.; Girotti, A. W.; Gollnick, S. O.; Hahn, S. M.; Hamblin, M. R.; Juzeniene, A.; Kessel, D.; Korbelik, M.; Moan, J.; Mroz, P.; Nowis, D.; Piette, J.; Wilson, B. C.; Golab, J. Photodynamic therapy of cancer: an update. *CA−Cancer J. Clin.* **2011**, *61*, 250−281.

(12) Musiol, R.; Serda, M.; Polanski, J. Prodrugs in Photodynamic Anticancer Therapy. *Curr. Pharm. Des.* **2011**, *17*, 3548−3559.

(13) Langer, S.; Abels, C.; Botzlar, A.; Pahernik, S.; Rick, K.; Szeimies, R. M.; Goetz, A. E. Active and higher intracellular uptake of 5-aminolevulinic acid in tumors may be inhibited by glycine. *J. Invest. Dermatol.* **1999**, *112*, 723−728.

(14) Ohgari, Y.; Nakayasu, Y.; Kitajima, S.; Sawamoto, M.; Mori, H.; Shimokawa, O.; Matsui, H.; Taketani, S. Mechanisms involved in delta-aminolevulinic acid (ALA)-induced photosensitivity of tumor cells: relation of ferrochelatase and uptake of ALA to the accumulation of protoporphyrin. *Biochem. Pharmacol.* **2005**, *71*, 42−49.

(15) Pye, A.; Curnow, A. Direct comparison of delta-aminolevulinic acid and methyl-aminolevulinate-derived protoporphyrin IX accumulations potentiated by desferrioxamine or the novel hydroxypyridinone iron chelator CP94 in cultured human cells. *Photochem. Photobiol.* **2007**, *83*, 766−773.

(16) Tan, W. C.; Krasner, N.; O'Toole, P.; Lombard, M. Enhancement of photodynamic therapy in gastric cancer cells by removal of iron. *Gut* **1997**, *41*, 14−18.

(17) Blake, E.; Curnow, A. The hydroxypyridinone iron chelator CP94 can enhance PpIX-induced PDT of cultured human glioma cells. *Photochem. Photobiol.* **2010**, *86*, 1154−1160.

(18) Basu, U.; Khan, I.; Hussain, A.; Kondaiah, P.; Chakravarty, A. R. Photodynamic effect in near-IR light by a photocytotoxic iron(III) cellular imaging agent. *Angew. Chem., Int. Ed.* **2012**, *51*, 2658−2661.

(19) Vurusaner, B.; Poli, G.; Basaga, H. Tumor suppressor genes and ROS: complex networks of interactions. *Free Radical Biol. Med.* **2012**, *52*, 7−18.

(20) Moan, J.; Bech, O.; Gaullier, J. M.; Stokke, T.; Steen, H. B.; Ma, L. W.; Berg, K. Protoporphyrin IX accumulation in cells treated with 5-aminolevulinic acid: dependence on cell density, cell size and cell cycle. *Int. J. Cancer* **1998**, *139*, 134−139.

(21) Chou, T. Theoretical basis, experimental design, and computerized simulation of synergism and antagonism in drug combination studies. *Pharmacol. Rev.* **2006**, *58*, 621−681.

(22) Bindslev, N. *Drug-Acceptor Interactions*; Co-Action Publishing: Sweden, 2009.

(23) Berg, K.; Anholt, H.; Bech, O.; Moan, J. The influence of iron chelators on the accumulation of protoporphyrin IX in 5-amino-laevulinic acid-treated cells. *Br. J. Cancer* **1996**, *74*, 688−697.

(24) Bech, O.; Phillips, D.; Moan, J.; MacRobert, A. J. A hydroxypyridinone (CP94) enhances protoporphyrin IX formation in 5-aminolaevulinic acid treated cells. *J. Photochem. Photobiol. B* **1997**, *41*, 136−144.

(25) Kemmner, W.; Wan, K.; Rüttinger, S.; Ebert, B.; Macdonald, R.; Klamm, U.; Moesta, K. T. Silencing of human ferrochelatase causes abundant protoporphyrin-IX accumulation in colon cancer. *FASEB J.* **2008**, *22*, 500−509.

(26) Moesta, K. T.; Ebert, B.; Handke, T.; Nolte, D.; Nowak, C.; Haensch, W. E.; Pandey, R. K.; Dougherty, T. J.; Rinneberg, H.; Schlag, P. M. Protoporphyrin IX occurs naturally in colorectal cancers and their metastases. *Cancer Res.* **2001**, *61*, 991−999.